Performance Analysis of Secure Cooperative Non Orthogonal Multiple Access and Hybrid Energy Harvesting in Vehicular Network

Opel N. Mbanzabugabo, Charles Kabiri, Kayalvizhi Jayavel and Louis Sibomana

***Abstract*—Improving the connectivity, security, and throughput of near and far vehicles in cooperative non-orthogonal multiple access (C-NOMA) communication with energy-constrained relays remains challenging, especially in the presence of eavesdropping E attacks. Existing works consider a single energy harvesting (EH) without a direct link (DL) between the base station (BS) and users, thus limiting the performance for both near and far users. To address the above challenges, this study proposes a hybrid EH and secure cooperative NOMA (HSC-NOMA) framework. The near user harvests energy from the received signal and operates as an energy-constrained relay to assist the far user. In contrast, the far user employs selection combining (SC) to select the strongest signal from direct and relayed links. Closed-form expressions for outage probability (OP), secrecy outage probability (SOP), and throughput (T) are derived under perfect successive interference cancellation (SIC). Numerical results illustrate that the proposed framework improves the performance of both near and far users. Outage probabilities of around 0.003 and 0.002 are achieved for the near and far vehicles, respectively, while secrecy outage probabilities are reduced to about 0.020 and 0.090. Furthermore, the proposed approach achieves improved throughput for both vehicles. It attains a higher system throughput of nearly 0.6 (normalized value), outperforming conventional time-switching-only, power-splitting-only, and cooperative NOMA schemes without a direct link.**

***Index Terms*—Non-orthogonal multiple access (NOMA), Hybrid energy harvesting (H EH), Secrecy outage probability (SOP), Sustainable development goals 9 (SDG 9): industry, innovation and infrastructure.**

Open License: CC-BY-NC-ND

I. Introduction

Non-orthogonal multiple access (NOMA) was developed for 5th generation (5G) and beyond wireless networks to improve spectral efficiency in massive connectivity networks [1-3]. Conversely, compared with traditional orthogonal multiple access (OMA) methods, cooperative non-orthogonal multiple access (C-NOMA) allows users to share the same resource using power-domain superposition while considering cooperative mode [4-6]. Recent research in [3-5] has highlighted the imbalance in the signal-to-interference-plus-noise ratio (SINR) between near and far vehicles. Typically, far vehicles experience lower SINR than near vehicles. Furthermore, as discussed in [6-8], reducing the disparity in data transmission rates requires allocating a larger portion of power to the far vehicle [5]. However, such a power allocation process may reduce the near vehicle's performance. To improve the data rate of cell-edge vehicles while maintaining fairness, cooperative relaying can be an effective solution [9-15].

As shown in [15-17], relaying systems are energy-constrained and may quickly deplete their available power in the absence of an external energy source. Energy harvesting (EH) has therefore emerged as an important technique in 5G and beyond networks, particularly for energy-limited systems, to improve operational efficiency [16-19]. Two adopted EH techniques are power splitting (PS) and time switching (TS) [18]. The TS energy harvesting (TS EH) alternates between EH and information-decoding (ID) phases. In contrast, PS energy harvesting (PS EH) divides the received signal into power levels, enabling concurrent energy harvesting and information decoding. As demonstrated in [19], the TS protocol performs well at lower transmitted power, whereas PS is more effective at high transmitted power [19]. Considering the benefits of both techniques, hybrid energy harvesting (H EH) integrates both TS and PS protocols, yielding improved performance across diverse conditions. This hybrid scheme improves system efficiency and outperforms individual TS and PS protocols, particularly for energy-limited vehicular relays [19].

As shown in [20-22], the authors examined cooperative NOMA with energy harvesting via PS or TS methods (or without any protocol), considering the direct link to a far vehicle from the base station. Nonetheless, they overlooked an H EH method, hence constraining the system's adaptability to fluctuating energy and channel conditions in vehicle environments. According to [23-26], the authors examined a cooperative NOMA scenario, in which the relay is an unmanned aerial vehicle (UAV) that utilizes simultaneous wireless information and power transfer to transmit information. The authors exclude a link between the BS and the far vehicle, constraining potential diversity and reducing robustness in poor channel conditions. As reported in [26-33], the authors studied cooperative NOMA with energy harvesting using either the PS or TS protocol, assuming that the far user is served only via a relay with no direct link from the base station. However,

O. N. Mbanzabugabo, C. Kabiri, and K. Jayavel are with the African Center of Excellence in Internet of Things (ACEIoT), University of Rwanda, Kigali. O. N. Mbanzabugabo is also with Mobile Telephone Network Rwanda, Kigali, Rwanda, and K. Jayavel is also with Data Science and Artificial Intelligence, Creative Computing Institute, University of the Arts London, London, UK (e-mails: mbanzabugabo.ndakebuka_221030128@stud.ur.ac.rw; c.kabiri@ur.ac.rw; k.jayavel@arts.ac.uk).

L. Sibomana is with the National Council for Science and Technology, Kigali, Rwanda (e-mail: lsibomana@ncst.gov.rw).

the system's adaptability fails to capitalize on opportunities to enhance diversity, thereby limiting its reliability in dynamic vehicular situations. Referring to [31], the authors focused on secure communication in reconfigurable intelligent surface (RIS) assisted NOMA systems with two eavesdroppers, using deep reinforcement learning, often neglecting communication liking the base station and vehicles. This oversight induces excessive dependence through the RIS-assisted pathway, which is vulnerable to signal degradation. Similarly, authors in [32] studied full-duplex cooperative NOMA networks with multiple eavesdroppers, and the system still didn't perform well even with deep learning techniques. Note that the link between the base station and the user was excluded. Following [32-34], the authors proposed an analytical framework for cooperative NOMA in Internet of Things (IoT) wireless communication. They focused on improving energy efficiency, outage probability, and throughput, while ignoring the secrecy outage probability. Per [35], the authors examined traditional security approaches, namely cryptographic protocols, for preventing unauthorized access by eavesdroppers. However, such security mechanisms are often computationally expensive, complex to implement, and still exposed to attacks. Physical layer security (PLS) is recommended to strengthen system security as it provides additional security information for monitoring communication systems by leveraging the physical-layer dynamics of wireless channels without requiring secret-key distribution [35]. In references [36-38], the authors refer to cooperative NOMA with a full-duplex relaying system and analyzed the secrecy for performance purposes. Using power-domain non-orthogonal multiple access (P-NOMA) with pure EH improved secrecy capacity. The study in [37] introduces a control-jammer (CJ) to enhance security in a decode-and-forward relay-assisted NOMA network. This proposed CJ scheme effectively protects the privileged information against eavesdropping. Specifically, the work in [37] reduces the secrecy outage probability (SOP) with a power constraint. The authors in [39-44] investigated relay-assisted C-NOMA networks in the downlink, where either amplify-and-forward (AF) or decode-and-forward (DF) relays are used to transmit information from the base station to two users in the presence of an eavesdropper. While the AF relaying strategy increases the received SINR, its reliability performance remains inferior to that of DF relaying due to the noise amplification. In reference [45], the authors show that imperfect successive interference cancellation (SIC) leads to residual interference at the near user in downlink C-NOMA systems with decode and forward (DF) relaying. This residual interference degrades the near-user's signal decoding performance, thereby increasing the secrecy outage probability and reducing the system's secrecy performance [45]. This observation highlights the need to optimize successive interference cancellation (SIC) and power allocation. However, the study is limited by its assumption of fixed SIC parameters and the lack of analysis of advanced strategies. In [46], the authors examine RIS-assisted NOMA systems with an on–off control method to adapt to RIS deviations and improve the secrecy outage probability [23-27].

Although cooperative NOMA has been extensively studied, as indicated in the literature review, many studies rely on simplistic assumptions that present limitations. A common simplification is the assumption that the far vehicle is served only via a relay, ignoring the link between the BS and the far vehicle [28-34]. Many studies address PS and TS protocols independently or omit energy harvesting, thereby restricting the system's ability to respond to energy fluctuations and degrading overall performance as illustrated in [20-22]. Moreover, physical-layer security for C-NOMA under the influence of eavesdroppers (E) has been investigated [35-38]. However, these works neglect the direct transmission or relaying links. The impact of direct transmission in cooperative NOMA was discussed in [20-22], but hybrid energy harvesting and security were not jointly considered. Therefore, the combined effect of hybrid energy harvesting, direct transmission, and selection combining in secure cooperative NOMA systems remains insufficiently explored.

To address the limitations mentioned above, this work proposes a more comprehensive HSC-NOMA framework that includes direct link connectivity, a hybrid EH scheme integrating PS and TS protocols, and the slow-fading channel assumption. Furthermore, physical layer security has been introduced to prevent eavesdropping. Analytical formulations for outage probability (OP), secrecy outage probability (SOP), and throughput (T) are formulated under perfect SIC, showing improved reliability, security, and spectral efficiency.

The following are the major contributions of this study:

1) To propose the HSC-NOMA framework, which integrates cooperative NOMA, hybrid energy harvesting (H EH), and direct links between the base station and vehicles in the presence of an eavesdropper. The near user acts as a relay, and a selection combining (SC) is applied at the far user to enhance the performance.
2) To develop an analytical framework and to derive closed-form expressions for the outage probability (OP), secrecy outage probability (SOP), and throughput (T) for near and far vehicles and under perfect successive interference cancellation (SIC). The analysis jointly considers hybrid energy harvesting (H EH), cooperative relaying, and direct links, thereby enabling the system performance.
3) To benchmark the proposed HSC-NOMA framework against conventional baseline schemes and demonstrate significant performance gains for both near and far users. For transmitted power of 16 dBm or higher, numerical findings show that the proposed framework achieves outage probabilities (OPs) of 0.003 and 0.002 for the near and far vehicles, respectively. In contrast, the secrecy outage probabilities (SOP) are reduced to around 0.020 for the near vehicle and 0.090 for the far vehicle. Moreover, the proposed scheme achieves a higher system throughput (T) of nearly 0.6 (normalized value), outperforming time-switching-only, power-splitting-only, and cooperative NOMA schemes without direct links.

The work is structured as follows. Section II introduces the system model. Section III provides the performance analysis. Section IV presents the results analysis and discussion. Finally,

Section V concludes the work and proposes future research.

II. System model

As illustrated in Fig. 1, a downlink cooperative NOMA (C-NOMA) communication system is considered, where the base station (BS) communicates with a near vehicle (V_1) and a far vehicle (V_2). Note that an eavesdropper (E) is connected to BS and V_1. All nodes have a single antenna and use half-duplex (HD) mode. The wireless links BS–V_1, BS–V_2, V_1–V_2, BS–E, and V_1–E have the following channel h_{sn}, h_{sf}, h_{nf}, h_{se}, and h_{ne} respectively [3], and note that each channel is supposed to experience Rayleigh fading. Therefore, broadcast links with channel coefficient h_k with zero mean and average channel gains λ_k for $k \in \{sn, sf, se\}$ are taken into account [4], [5]. Additionally, point-to-point links with channel coefficient h_i with zero mean and average channel gains λ_i for $i \in \{nf, ne\}$ [4]. Thus, the corresponding channel gains $|h_k|^2$ and $|h_i|^2$ follow an exponential distribution, illustrated by their probability density functions (PDF) [6].

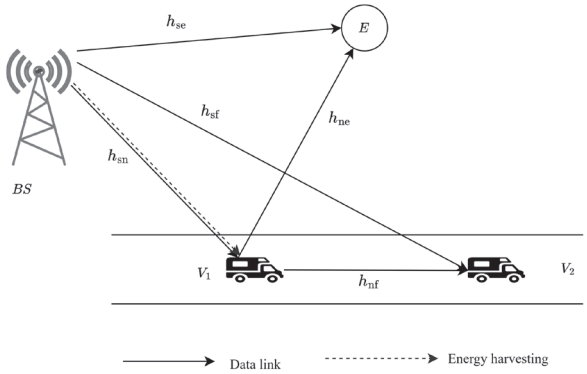


Fig. 1: System model

A. Energy harvesting

The broadcast signals from BS to vehicles V_1, V_2 and eavesdrop (E) is given by [7]:

$$y_k = \left(\sqrt{p_n P_s}x_N + \sqrt{p_f P_s}x_F\right)h_k + N_k \tag{1}$$

where x_N and x_F are the transmit signals, from vehicles V_1 and V_2, respectively. Note that $h_k \sim \mathcal{CN}(0, \lambda_k)$ and $N_k \sim \mathcal{CN}(0, \sigma_k^2)$, p_n and p_f denote the power allocation coefficient for near and far vehicles, respectively. With $p_n + p_f = 1$ and P_s is the total transmit power from the base station [7].
For simplification, it can be assumed that N_{sn} = N_{sf} = N_{se} = N_c. The signal received by near vehicle V_1 is:

$$y_{sn} = \left(\sqrt{1-\varepsilon}\right)\left(\sqrt{p_n P_s}x_N + \sqrt{p_f P_s}x_F\right)h_{\text{sn}} + N_{sn} \tag{2}$$

where $N_c \sim \mathcal{CN}(0, \sigma^2)$ and ε is PS energy harvesting factor. The received signal y_{nf} of the far vehicle from the cooperative link can be expressed as:

$$y_{nf} = \sqrt{P_v}h_{\text{nf}}\hat{x}_F + N_{nf} \tag{3}$$

where $\hat{x}_F$ is an estimated value of x_F and N_{nf} is the additive white Gaussian noise equal to N_c for simplification. The power P_v is harvested from V_1 to V_2 and $\hat{x}_F$ is the transmitted signal from V_1 to V_2 in relay link. The signal y_{E2}, received by eavesdrop from vehicle V_1 is

$$y_{ne} = \sqrt{P_v}h_{\text{ne}}\hat{x}_F + N_{ne}. \tag{4}$$

Note that N_{ne} is also the additive white Gaussian noise equal to N_c, for simplification. The proposed hybrid protocol has three steps for communication. The first step concerns the TS with θT as an interval and where the relay V_1 receives energy from the BS. Note that θ is the time switching coefficient with $0 < \theta < 1$ and T is the total transmission block time. Second step within $\frac{(1-\theta)T}{2}$ where V_1 use PS energy harvesting with factor $\varepsilon \in (0, 1)$ with $1-\varepsilon$ to decode the information. The last step $\frac{(1-\theta)T}{2}$ is related to the transmission of a message from a near vehicle to a far vehicle. The hybrid energy harvesting (H EH) is given by the sum of energy from TS and PS,

$$E_h = \eta\,|h_{\text{sn}}|^2\,P_s\theta T + \eta\varepsilon\,|h_{\text{sn}}|^2\,P_s\frac{(1-\theta)T}{2} \tag{5}$$

where η is a factor defining the energy conversion. Hybrid power harvesting P_v at the near vehicle, is derived as

$$P_v = \frac{E_h}{(1-\theta)\frac{T}{2}}. \tag{6}$$

Introducing (5) into (6), P_v can be defined as

$$P_v = |h_{\text{sn}}|^2\,P_s b, \tag{7}$$

where $b = 2V + \eta\varepsilon$ and $V = \frac{\eta\theta}{1-\theta}$.

B. Signal-to-interference-plus-noise ratio

Following the NOMA principle, the receiver at V_1 applies successive interference cancellation (SIC) by first decoding the message of vehicle V_2, thereafter subtracting it from (2) to recover its own message. According to (2), the SINR (Γ_{a}) at near vehicle for recovering x_F, is defined by

$$\Gamma_{\text{a}} = \frac{(1-\varepsilon)p_f\psi|h_{\text{sn}}|^2}{(1-\varepsilon)p_n\psi|h_{\text{sn}}|^2 + 1} \tag{8}$$

where $\psi = \frac{P_s}{\sigma^2}$.
The received SINR (Γ_{SN}) at the near user to decode its own information x_N can be defined as

$$\Gamma_{\text{SN}} = (1-\varepsilon)p_n\psi|h_{\text{sn}}|^2. \tag{9}$$

From (1), the received SINR (Γ_{b}) at V_2 from direct link, is derived as

$$\Gamma_{\text{b}} = \frac{p_f\psi|h_{\text{sf}}|^2}{p_n\psi|h_{\text{sf}}|^2 + 1}. \tag{10}$$

From (3), the received SINR (Γ_{NF}) at far vehicle for detecting the signal x_F from near vehicle, can be defined as

$$\Gamma_{\text{NF}} = \frac{P_v|h_{\text{nf}}|^2}{\sigma^2}. \tag{11}$$

Putting (7) into (11),

$$\Gamma_{\text{NF}} = \psi|h_{\text{sn}}|^2|h_{\text{nf}}|^2(2V + \eta\varepsilon). \tag{12}$$

Using the selection combining (SC) method, the achievable SINR of the far vehicle can be written as

$$\Gamma_{\mathrm{F}} = \max\left\{\Gamma_{\mathrm{b}}, \min\left\{\Gamma_{\mathrm{a}}, \Gamma_{\mathrm{NF}}\right\}\right\}. \tag{13}$$

During the transmission of the message from BS to V_1, E has access to information x_F as well as x_N, and their SINR are respectively defined from (1),

$$\Gamma_{\mathrm{c}} = \frac{p_f \psi |h_{\mathrm{se}}|^2}{p_n \psi |h_{\mathrm{se}}|^2 + 1}, \tag{14}$$

$$\Gamma_{\mathrm{d}} = p_n \psi |h_{\mathrm{se}}|^2. \tag{15}$$

While V_1 transmits x_F to V_2, E has access to this information and the SINR (Γ_{e}) at E can be computed from (4) and (7).

$$\Gamma_{\mathrm{e}} = \psi |h_{\mathrm{ne}}|^2 |h_{\mathrm{sn}}|^2 (2V + \eta\varepsilon). \tag{16}$$

III. Performance Analysis

The proposed HSC-NOMA framework is evaluated by the following main metrics: outage probability (OP), secrecy outage probability (SOP), and throughput (T).

A. Outage probability of vehicle V_1

The outage probability of the near vehicle occurs when either x_F can't be recovered from SIC or the signal x_F is decoded successfully at the far user side while x_N is not decoded correctly. Thus, the OP of the near vehicle can be computed as follows:

$$P_{n\mathrm{out}} = Pr\Big(\Gamma_{\mathrm{a}} < \gamma_2\Big) + Pr\Big(\Gamma_{\mathrm{a}} \geq \gamma_2, \Gamma_{SN} < \gamma_1\Big). \tag{17}$$

Considering (8) and (9) in (17), we have:

$$\begin{aligned} P_{n\mathrm{out}} =& Pr\left[\frac{\vartheta p_f \psi |h_{\mathrm{sn}}|^2}{\vartheta p_n \psi |h_{\mathrm{sn}}|^2 + 1} < \gamma_2\right] \\ &+ Pr\left[\frac{\vartheta p_f \psi |h_{\mathrm{sn}}|^2}{\vartheta p_n \psi |h_{\mathrm{sn}}|^2 + 1} \geq \gamma_2, \right. \\ &\left. \vartheta p_n \psi |h_{\mathrm{sn}}|^2 < \gamma_1\right] \end{aligned} \tag{18}$$

where signal to noise thresholds $\gamma_1 = 2^{\frac{2R_1}{(1-\theta)}} - 1$, and $\gamma_2 = 2^{\frac{2R_2}{(1-\theta)}} - 1$ are required to successfully recover the signals x_N and x_F, respectively. Transmission rates for vehicles V_1 and V_2 are also R_1 and R_2, respectively, and note that $\vartheta = 1 - \varepsilon$. Following some mathematical changes and $P_{n\mathrm{out}}$ in (18) can be further expressed as

$$P_{n\mathrm{out}} = \begin{cases} 1 - \exp\left(\frac{-\gamma_1}{\vartheta\psi p_n \lambda_{sn}}\right), & \gamma_2 < \frac{p_f}{p_n} \\ \text{and } \mu_a < \frac{\gamma_1}{\vartheta\psi p_n}, & \\ 1 - \exp\left(\frac{-\gamma_2}{\vartheta\psi(p_f - p_n\gamma_2)\lambda_{sn}}\right), & \gamma_2 < \frac{p_f}{p_n} \\ \text{and } \mu_a \geq \frac{\gamma_1}{\vartheta\psi p_n}, & \\ 1, & \gamma_2 \geq \frac{p_f}{p_n} \\ \text{and } \forall\gamma_1. & \end{cases} \tag{19}$$

B. Outage probability of vehicle V_2

The outage probability of V_2 can be expressed as follows.

$$P_{f\mathrm{out}} = Pr\Big(\max\left\{\Gamma_{\mathrm{b}}, \min\left\{\Gamma_{\mathrm{a}}, \Gamma_{NF}\right\}\right\} < \gamma_2\Big) \tag{20}$$

Putting (8), (10) and (11) in (20), $P_{f_{\mathrm{out}}}$ becomes,

$$\begin{aligned} P_{f\mathrm{out}} = Pr\Bigg\{&\max\left[\frac{p_f \psi |h_{\mathrm{sf}}|^2}{p_n \psi |h_{\mathrm{sf}}|^2 + 1}, \right. \\ &\left. \min\left(\frac{\vartheta p_f \psi |h_{\mathrm{sn}}|^2}{\vartheta p_n \psi |h_{\mathrm{sn}}|^2 + 1}, \psi |h_{\mathrm{sn}}|^2 |h_{\mathrm{nf}}|^2 (2V + \eta\varepsilon)\right)\right] < \gamma_2\Bigg\} \end{aligned} \tag{21}$$

Consequently, P_{fout} can be rewritten, with conditions: $X = x = |h_{\mathrm{sn}}|^2$, $Y = |h_{\mathrm{sf}}|^2$ and $Z = |h_{\mathrm{nf}}|^2$.

$$\begin{aligned} P_{f\mathrm{out}} = \int_0^\infty Pr\Bigg\{&\max\left[\frac{p_f \psi Y}{p_n \psi Y + 1}, \right. \\ &\left. \min\left(\frac{\vartheta p_f \psi x}{\vartheta p_n \psi x + 1}, \psi x Z (2V + \eta\varepsilon)\right)\right] \\ &< \gamma_2\Bigg\} f_X(x)\, dx \end{aligned} \tag{22}$$

Similarly, as shown in (19), when $\gamma_2 \geq \frac{p_f}{p_n}$, then $P_{f_{\mathrm{out}}} = 1$. For $\gamma_2 < \frac{p_f}{p_n}$, $P_{f_{\mathrm{out}}}$ can be defined as

$$\begin{aligned} P_{f\mathrm{out}} = 1 - \int_{\omega_a}^\infty Pr\Bigg(&\max\left(\frac{p_f \psi Y}{p_n \psi Y + 1}, \right. \\ &\left. \psi x Z (2V + \eta\varepsilon)\right) \geq \gamma_2\Bigg) f_X(x)\, dx \end{aligned} \tag{23}$$

where $\omega_a = \frac{\gamma_2}{\vartheta\psi(p_f - \gamma_2 p_n)}$.

Considering the maximum rule and applying the complement probability theorem (23) becomes,

$$\begin{aligned} P_{f\mathrm{out}} =& 1 - \int_{\omega_a}^\infty \Bigg[1 - Pr\left(\frac{p_f \psi Y}{p_n \psi Y + 1} < \gamma_2\right) \\ &\times \Pr(\psi x Z (2V + \eta\varepsilon) < \gamma_2)\Bigg] f_X(x)\, dx. \end{aligned} \tag{24}$$

Through the use of the cumulative distribution function (CDF) and the probability density function (PDF) of the variable X, (24) can be written,

$$\begin{aligned} P_{f\mathrm{out}} =& 1 - \frac{1}{\lambda_{sn}} \int_{\omega_a}^\infty \Bigg[1 - \left(1 - \exp\left(-\frac{\omega_b}{\lambda_{sf}}\right)\right) \\ &\times \left(1 - \exp\left(-\frac{\gamma_2}{\lambda_{nf} c x}\right)\right)\Bigg] \\ &\times \exp\left(-\frac{x}{\lambda_{sn}}\right) dx. \end{aligned} \tag{25}$$

with $\omega_b = \frac{\gamma_2}{\psi(p_f - \gamma_2 p_n)}$ and $c = \psi(2V + \eta\varepsilon)$ (for hybrid energy harvesting) and where $V = 0$ and $\varepsilon = 0$ correspond to power

splitting and time switching protocols, respectively [6]. After some manipulation, $P_{f_{\text{out}}}$ is given by the following expression,

$$P_{f\text{out}} = 1 - \exp\left(-\frac{\omega_a}{\lambda_{sn}}\right) + \left[1 - \exp\left(-\frac{\omega_b}{\lambda_{sf}}\right)\right] \times \left[\exp\left(-\frac{\omega_a}{\lambda_{sn}}\right) - \frac{1}{\lambda_{sn}} \int_{\mu_a}^{\infty} \exp\left(-\frac{x}{\lambda_{sn}} - \frac{\gamma_2}{\lambda_{nf} c x}\right) dx\right]. \quad (26)$$

Due to the analytical constraints provided by Rayleigh fading and the interaction of hybrid energy harvesting with cooperative NOMA, there is no closed-form expression for the integral in (26). Thus, numerical approaches are used for assessment, and the findings are verified using Monte Carlo simulations.

C. Secrecy outage probability of vehicle V_1

The SOP shows the probability that an E successfully decodes the transmitted message. The amount of secure communication that may be performed when an E is present is defined as the secrecy capacity (SC_n). It can be formulated for V_1 as

$$SC_n = |C_{V_n} - C_E^n|^+ = \frac{1-\theta}{2} \log_2\left(\frac{1+\Gamma_{\text{SN}}}{1+\Gamma_{\text{d}}}\right) \quad (27)$$

where $C_{V_n} = \frac{1-\theta}{2}\log_2(1+\Gamma_{\text{SN}})$ and $C_E^n = \frac{1-\theta}{2}\log_2(1+\Gamma_{\text{d}})$, C_{V_n} is the link capacity of V_1 and C_E^n is the link capacity of E to access x_N information. The SOP of at vehicle V_1 is defined as

$$S_{OP_1} = Pr(SC_n < R_3) \quad (28)$$

with R_3 denoting the secrecy target rate threshold for decoding x_N. Putting (27) into (28), the following is obtained,

$$S_{OP_1} = Pr\left(\frac{1-\theta}{2} \log_2\left(\frac{1+\Gamma_{\text{SN}}}{1+\Gamma_{\text{d}}}\right) < R_3\right) \quad (29)$$

$$= 1 - Pr\left(\left[\frac{1+\Gamma_{\text{SN}}}{1+\Gamma_{\text{d}}}\right] > \phi_1\right) \quad (30)$$

where $\phi_1 = 2^{\frac{2R_3}{1-\theta}}$.
Inserting expressions (9) and (15) in (30),

$$S_{OP_1} = 1 - Pr\left(\left[\frac{1+(1-\varepsilon)p_n\psi|h_{\text{sn}}|^2}{1+p_n\psi|h_{\text{se}}|^2}\right] > \phi_1\right) \quad (31)$$

$$= 1 - Pr\left(\left[(k_1|h_{\text{sn}}|^2 - k_2|h_{\text{se}}|^2)\right] > \phi_2\right) \quad (32)$$

where $\phi_2 = \phi_1 - 1$, $k_1 = p_n\psi(1-\varepsilon)$ and $k_2 = \phi_1 p_n \psi$.

Let us consider U as a function of two random variables $U = k_1|h_{\text{sn}}|^2 - k_2|h_{\text{se}}|^2$, and its CDF is,

$$F_U(u) = \int_0^{\infty} \int_0^{\frac{u+k_2 w}{k_1}} f_{XW}(x,w)\, dx\, dw$$

with $X = |h_{\text{sn}}|^2$, $W = |h_{\text{se}}|^2$ and for $u > 0$.
Using Leibniz's rule of integration, the PDF of the variable U may be defined as

$$f_U(u) = \int_0^{\infty} f_{XW}\left(\frac{u+k_2 w}{k_1}, w\right) dw. \quad (33)$$

With X and W as independent random variables, (33) can be expressed as

$$f_U(u) = \int_0^{\infty} f_X\left(\frac{u+k_2 w}{k_1}\right) f_W(w)\, dw = f_X(-u) * f_W(w). \quad (34)$$

With exponential distribution random variables applied in (34), and after some computation, the PDF of U is reduced to

$$f_U(u) = k_5 \exp\left(\frac{-u}{k_4}\right) \quad (35)$$

with $k_3 = k_2\lambda_{se}$, $k_4 = k_1\lambda_{sn}$ and $k_5 = k_1/(k_3+k_4)$.
From expression (32),

$$S_{OP_1} = 1 - \int_{\phi_2}^{\infty} f_U(u)\, du. \quad (36)$$

Substituting (35) into (36), and after some calculation, the secrecy outage probability of vehicle V_1 is finally expressed as

$$S_{OP_1} = 1 - \frac{k_5}{k_4}\exp(-k_4\phi_2). \quad (37)$$

D. Secrecy outage probability of vehicle V_2

Let us consider the high-level signal for reducing the complexity of the proposed method, and the maximum ratio combining (MRC) is taken into account. With (10), (11), (14), and (16), the derivation of the SC_f for the far vehicle can be formulated as follows.

$$SC_f = \left|C_{V_f} - C_E^f\right|^+ = \frac{1-\theta}{2}\log_2\left(\frac{1+\Gamma_{\text{b}}+\Gamma_{\text{NF}}}{1+\Gamma_{\text{c}}+\Gamma_{\text{e}}}\right) \quad (38)$$

in which C_{V_f} and and C_E^f indicate the link capacity of V_2 and the link capacity of E to access x_F information, respectively. Thus, the SOP of vehicle V_2 can be defined,

$$S_{OP_2} = Pr(SC_f < R_4) \quad (39)$$

where R_4 is the required secrecy target rate to decode x_F. Based on (38) and (39), S_{OP_2} can be deduced as

$$S_{OP_2} = Pr\left(\left[\frac{1+\frac{p_f}{p_n}+\psi|h_{\text{sn}}|^2|h_{\text{nf}}|^2(2V+\eta\varepsilon)}{1+\frac{p_f}{p_n}+\psi|h_{\text{sn}}|^2|h_{\text{ne}}|^2(2V+\eta\varepsilon)}\right] < \delta_1\right)$$

$$= Pr\left(\left[\psi|h_{\text{sn}}|^2|h_{\text{nf}}|^2 b - \delta_1\psi|h_{\text{sn}}|^2|h_{\text{ne}}|^2 b\right] < \delta_2\right) \quad (40)$$

where δ_1 is the secrecy target threshold to decode x_F, $\delta_1 = 2^{\frac{2\tilde{R}_4}{1-\theta}}$ and $\delta_2 = \left(1 + \frac{p_f}{p_n}\right)(\delta_1 - 1)$.

$$S_{OP_2} = Pr\left(\left[q_1|h_{\text{sn}}|^2|h_{\text{nf}}|^2 - q_2|h_{\text{sn}}|^2|h_{\text{ne}}|^2\right] < \delta_2 \right) \quad (41)$$

where $q_1 = \psi b$ and $q_2 = \delta_1 b\psi$.

$$\begin{aligned} S_{OP_2} &= Pr\left([(q_1 Z - q_2 M)] < \frac{\delta_2}{X} \right) \\ &= \int_0^\infty \int_0^\infty \int_0^{\frac{\delta_2}{xq_1} + \frac{q_2 m}{q_1}} f_{XZM}(x, z, m)\, dx\, dz\, dm \end{aligned} \quad (42)$$

with $X = |h_{\text{sn}}|^2$, $Z = |h_{\text{nf}}|^2$, and $M = |h_{\text{ne}}|^2$. These random variables are independent; thus, (42) becomes,

$$S_{OP_2} = \int_0^\infty \int_0^\infty \int_0^{\frac{\delta_2}{xq_1} + \frac{q_2 m}{q_1}} f_X(x) f_Z(z) f_M(m)\, dx\, dz\, dm. \quad (43)$$

From (43), let us integrate with respect to z (I_1),

$$\begin{aligned} I_1 &= \int_0^{\frac{\delta_2}{xq_1} + \frac{q_2 m}{q_1}} f_Z(z)\, dz \\ &= 1 - exp\left[- \left(\frac{\delta_2}{xq_1\lambda_{nf}} + \frac{q_2 m}{q_1 \lambda_{nf}} \right) \right]. \end{aligned} \quad (44)$$

Similarly, when integrating with respect to m, the result is as follows,

$$\begin{aligned} I_2 &= \int_0^\infty \left[1 - \exp\left(- \frac{\delta_2}{xq_1\lambda_{nf}} - \frac{q_2 m}{q_1 \lambda_{nf}} \right) \right] f_M(m)\, dm, \\ &= \int_0^\infty \frac{1}{\lambda_{ne}} e^{-\frac{m}{\lambda_{ne}}}\, dm \\ &\quad - \frac{1}{\lambda_{ne}} \exp\left(- \frac{\delta_2}{xq_1\lambda_{nf}} \right) \int_0^\infty e^{-\frac{m}{\mu}}\, dm, \end{aligned} \quad (45)$$

where $\frac{1}{\mu} = \dfrac{q_1\lambda_{nf} + q_2\lambda_{ne}}{q_1\lambda_{nf}\lambda_{ne}}$.

After some mathematical manipulations, I_2 can be written as

$$I_2 = 1 - \frac{\lambda_{nf}\lambda_{ne} q_1}{q_1\lambda_{nf} + q_2} \frac{1}{\lambda_{ne}} e^{-\frac{\delta_2}{xq_1\lambda_{nf}}}. \quad (46)$$

Integrating with respect to x and referring to (44) and (46), the SOP of the far vehicle V_2 is given by [3],

$$S_{OP_2} = \left(1 - \frac{\lambda_{nf}\lambda_{ne} q_1}{q_1\lambda_{nf} + q_2} \frac{1}{\lambda_{ne}} e^{-\frac{\delta_2}{xq_1\lambda_{nf}}} \right) \int_0^\infty \frac{1}{\lambda_{sn}} e^{-\frac{x}{\lambda_{sn}}}\, dx,$$

$$S_{OP_2} = 1 - \frac{\lambda_{nf}\lambda_{ne} q_1}{q_1\lambda_{nf} + q_2} \frac{1}{\lambda_{ne}} \int_0^\infty \frac{1}{\lambda_{sn}} \exp\left(- \frac{x}{\lambda_{sn}} - \frac{\delta_2}{xq_1\lambda_{nf}} \right) dx.$$

With reference to [47, Eq. (3.324.1)], the above expression becomes,

$$S_{OP_2} = 1 - \frac{\lambda_{nf}\lambda_{ne} q_1}{q_1\lambda_{nf} + q_2} \frac{1}{\lambda_{ne}} \sqrt{\frac{4\delta_2}{q_1\lambda_{nf}\lambda_{sn}}} K_1 \sqrt{\frac{4\delta_2}{q_1\lambda_{nf}\lambda_{sn}}} \quad (47)$$

where K_1 is the modified Bessel function.

E. Throughput analysis

In this subsection, the downlink throughput for C-NOMA is analyzed,

$$T_n = (1 - P_{n\text{out}}) R_1 \quad (48)$$

$$T_f = (1 - P_{f\text{out}}) R_2 \quad (49)$$

where T_n and T_f are the throughput of vehicles V_1 and V_2 respectively. Expressions of P_{nout} and P_{fout} are given in (19) and (26), respectively.

IV. Numerical and Simulation Results

This section presents numerical results from Monte Carlo simulations using MATLAB and Python. The simulation parameters follow [23-25]. The normalized distance between the base station (BS) and near vehicle V_1 is set to 3, while the distance between the BS and far vehicle V_2 is 10. The power allocation ratio for the near vehicle and the power-splitting ratio are 0.1 and 0.3, respectively. The energy conversion for the energy harvesting (EH) is $\eta = 0.7$. The number of Monte Carlo realizations is 10^6, the bandwidth is $1\,\text{MHz}$, and the received noise power is around $-100\,\text{dBm}$. The target data rates for both vehicles are set to $0.3\,\text{bps/Hz}$. The numerical results match the simulations, validating the theoretical results. The outage probability is evaluated as a function of transmit power (dBm) under three baselines: without EH and without a direct link (DL), without EH but with a direct link, and with both EH and a direct link. The first two baselines are presented in Fig. 2, while the third scenario relative to the proposed method is illustrated in Fig. 3.

Fig. 2 shows that without a direct link and energy harvesting, the outage probability of the far vehicle degrades even with increased transmission power. Two scenarios are considered to reduce the outage probability (OP) for the far vehicle. Without the direct link, the outage probability of the far vehicle is very high and remains constant at 1, indicating the direct link's greatest contribution. When integrating the direct link, the outage probability (OP) of the far vehicle decreases from 1 to nearly 0.5 for a transmit power of 0 dBm. The outage probability drops below 0.1 when the transmit power increases from 0 to 20 dBm, which indicates a significant improvement of the proposed framework. The near and far vehicles achieve good performance at higher transmit power, even without energy harvesting. Their outage probabilities are very low and converge to zero. Particularly, for a near vehicle, a significant improvement is achieved, as its outage probability tends toward zero, even in the absence of direct or relay links and at lower transmit power. This is

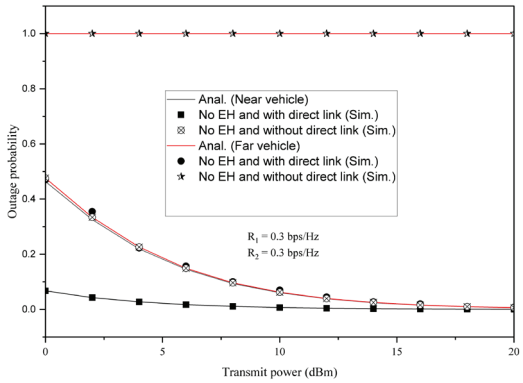


Fig. 2: Outage probability of near (N) and far (F) vehicles versus transmit power, with baseline consideration.

because no power is used for harvesting; all power is fully utilized for information transmission at the near vehicle.

As shown in Fig. 3, this scenario involves integrating cooperative NOMA with energy-harvesting considerations (e.g., TS, PS, and H EH). The outage probability of the far vehicle is lower than that of a near vehicle at low transmit power levels. The SINR of the near vehicle decreases because a portion of the power it receives intended for information transmission is diverted to energy-harvesting (EH) relaying. But for transmitted power greater than 16 dBm, the outage probability for all vehicles is around 0. When adjusting the PS and TS ratios to $\varepsilon = 0.2$ and $\theta = 0.1$, respectively, the performance of the proposed framework significantly improves compared to the system with PS or TS considered separately.

As shown in Fig. 4, the SOP for the near vehicle decreases across all EH-related schemes. The secrecy outage probability decreases while the transmitted power increases (from 0 to 20 dBm), demonstrating that higher transmit power improves the signal quality of legitimate users, whereas the eavesdropper. A lower data rate threshold corresponds to a lower SOP, whereas higher thresholds lead to larger SOP, particularly at low transmit power levels. Therefore, increasing transmit power improves the overall SOP performance regardless of the selected data-rate threshold.

As shown in Fig. 5, without EH, the far vehicle's SOP is very high, resulting in poor transmission performance. When the time-switching (TS) protocol is used, the SOP decreases with increasing transmit power; however, it remains higher than that of the power-splitting (PS) and hybrid schemes (HS). The TS energy-harvesting allocates a portion of its transmission time to harvesting, while reducing the time available for transmitting information. The performance of PS EH is improved by EH and information decoding, enabling more efficient energy use and a lower secrecy outage probability. By combining TS and PS, the hybrid scheme (HS) achieves the best secrecy performance, achieving the lowest SOP through all given transmit power values. This demonstrates that the hybrid approach improves the reliability and security for the far and near vehicles compared to conventional EH schemes and a baseline without EH. With the hybrid EH protocol, the proposed HSC-NOMA framework is more secure compared to TS and PS EH.

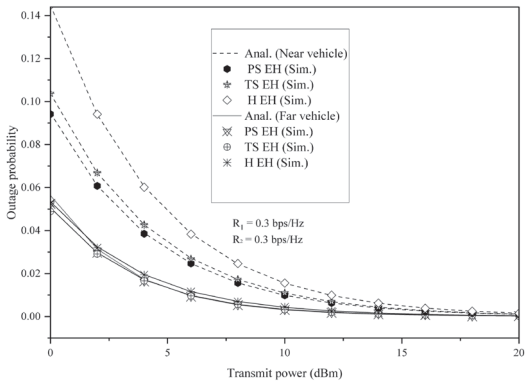


Fig. 3: Outage probability of near (N) and far (F) vehicles versus transmit power, with EH consideration.

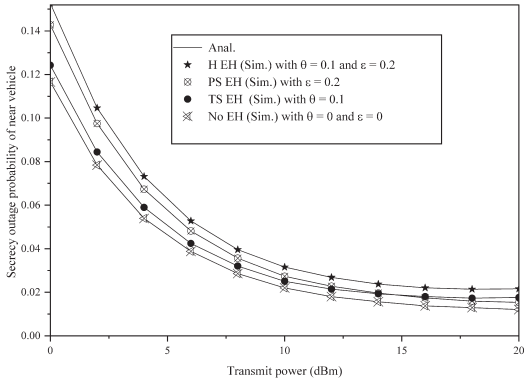


Fig. 4: SOP for near vehicle (N) versus transmit power.

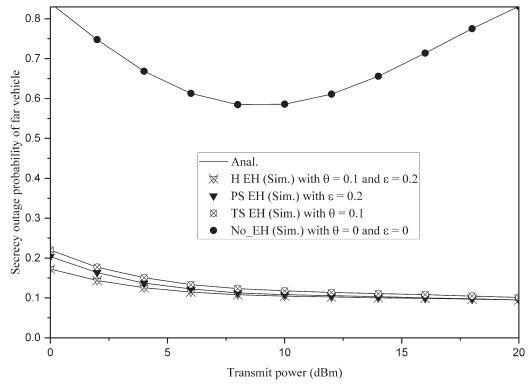


Fig. 5: SOP for far vehicle (F) versus transmit power.

As shown in Fig. 6, the consideration of a direct link between BS and the far vehicle reduces the secrecy outage probability (SOP) across all transmit power levels compared to the system without such a link. This improvement arises because V_2 benefits from selecting the stronger signal along the direct and cooperative paths, thereby improving the overall

secrecy outage probability. As a result, the direct link improves the network's security and reliability by providing an additional communication path to the far vehicle. Additionally, to

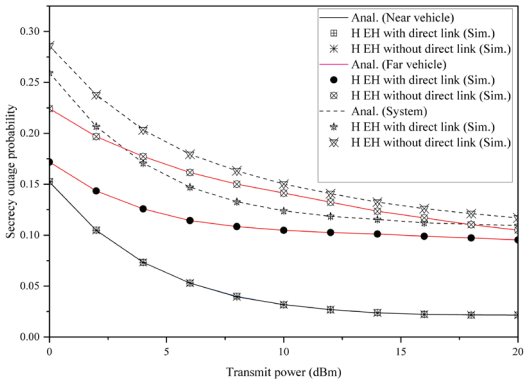


Fig. 6: SOP of near (N) vehicle, far (F) vehicle, and system (S) versus Transmit power (showing the positive impact of the link between BS and far user).

improve the overall system's performance, the hybrid energy harvesting (H EH) mode is employed with carefully selected parameter values of $\theta = 0.1$ and $\rho = 0.2$. At transmit power levels of 16.5 dBm and above, the secrecy outage probability (SOP) decreases to 0.025 for vehicle V_1 and 0.095 for vehicle V_2, demonstrating a significant improvement offered by the proposed HSC-NOMA framework.

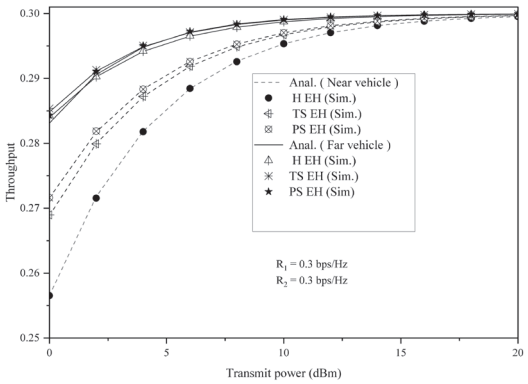


Fig. 7: Throughput of near vehicle and far vehicle versus transmit power.

As shown in Fig. 7, at transmit power levels above 16 dB, throughput increases for both near and far vehicles to approximately 0.30. At transmit power below 16 dBm, the far vehicle outperforms the near vehicle in throughput, indicating that the system performs well for both vehicles at lower or higher transmit power.

V. Conclusion and Future Work

The proposed HSC-NOMA framework integrates a secure cooperative NOMA with hybrid energy harvesting and a direct link, in which the near vehicle operates as an energy-harvesting relay. The results show significant improvement for the overall system (near and far vehicles). The proposed HSC-NOMA framework improves the performance by reducing the outage probability to around 0.003 and 0.002 for near and far vehicles, respectively. These results indicate that the proposed method improves reliability compared to conventional baselines, with TS and/or PS, without a direct link. The secrecy outage probability decreased to about 0.020 for the near user and 0.090 for the far user, showing improved resistance against eavesdropping. The HSC-NOMA framework also improves system throughput to around 0.6 (normalized value). Future work will focus on dynamic optimization of TS and PS ratios in real time to improve the performance.

Data Availability Statement: All data supporting this study are included within this research; no external datasets were used.

References

[1] Q. S. Ahmad et al., "Achievable Sum Rate Analysis for Moving Relay-Assisted Cooperative NOMA System over Rician Fading Channels," *IEEE Access*, vol. 13, pp. 29778-29788, Feb. 2025.

[2] K. M. Rabie, "Performance Analysis of Cooperative NOMA Networks over Compound Fading Channels," *IEEE Access*, vol. 4, pp. 1-10, May 2026.

[3] M. Imran et al., "Investigating Low Latency Communications With Link-Layer Rate of NOMA Under Nakagami-m Fading Channel in Finite Blocklength Regime," *IEEE Access*, vol. 13, pp. 24237-24250, Jan. 2025.

[4] A. Amhaz et al., "Integrated Sensing and Communication: NOMA vs Cooperative NOMA," in *Proc. IEEE Global Communications Conference: Next-Generation Networking and Internet*, Kuala Lumpur, Malaysia, Dec. 2023, pp. 407-412.

[5] M.C. Mayarakaca and B.M. Lee, "A Survey on Non-Orthogonal Multiple Access for Unmanned Aerial Vehicle Networks: Machine Learning Approach," *IEEE Access*, vol. 12, pp. 51138-51165, Mar. 2024.

[6] M. Imran et al., "Investigating Low Latency Communications With Link-Layer Rate of NOMA Under Nakagami-m Fading Channel in Finite Blocklength Regime," *IEEE Access*, vol. 13, pp. 24237-24250, Jan. 2025.

[7] W. Huang et al., "Energy Efficiency in Hybrid NOMA-MEC Networks," *IEEE Trans. wireless Commun.*, pp. 1-14, Mar. 2025.

[8] Y. Pramitarini et al., "Opportunistic Scheduling Scheme to Improve Physical-Layer Security in Cooperative NOMA System: Performance Analysis and Deep Learning Design," *IEEE Access*, vol. 12, pp. 58454-58472, Apr. 2024.

[9] S. P. Indraganti et al., "Survey of Cooperative NOMA for Beyond 5G: State-of-the-Art, Applications and Research Directions," *IEEE Open J. Commun. Soc.*, pp. 40-94, Jan. 2026.

[10] B. Lall et al., "Performance Analysis of Downlink Cooperative User Relaying FD/HD NOMA Over Nakagami-m Fading Channels, " *IEEE Trans. Veh. Technol.*, vol. 73, no. 6, pp. 1-16, Feb. 2024.

[11] A. Mukherjee et al., "Performance of Novel Adaptive Schemes for Cognitive Full-Duplex Relaying-Based Downlink Cooperative NOMA, " *IEEE Trans. Veh. Technol.*, vol. 73, no. 6, pp. 3161-3179, May. 2023.

[12] A. Le et al., "Power Beacon and NOMA-Assisted Cooperative IoT Networks With Co-Channel Interference: Performance Analysis and Deep Learning Evaluation, " *IEEE Trans. Mob. Comput.*, vol. 23, no. 6, pp. 7270-7283, Jun. 2024.

[13] B. Zhuo et al., "P-NOMA for Pinching-Antenna Systems (PASS)," *IEEE Wireless Commun. Lett.*, vol. 15, no. 1, pp. 131-135, Mar. 2026.

[14] Y. Lou et al., "Sum Secrecy Rate Maximization in Movable Antenna-Assisted NOMA Secure Transmission Systems," *IEEE Trans. Wireless Commun.*, vol. 25, no. 1, pp. 13011-13024, Mar. 2026.

[15] A. Pradhan et al., "Enhancing Physical Layer Security of URLLC Using Artificial Noise in Full-Duplex Cooperative NOMA," *IEEE Trans. Veh. Technol.*, vol. 75, no. 1, pp. 1044–1056, Jan. 2026.

[16] A. S. Parihar et al., "On Performance of SWIPT Empowered NOMA-HetNet with Non-Linear Energy Harvesting," in *Proc. IEEE National Conference on Communications (NCC)*, Chennai, India, Apr. 2024, pp. 1-6.

[17] A. K. Baranwal, S. D. Roy and S. Kundu, "Performance Analysis of Full-Duplex Cooperative NOMA with Power-Time Splitting Based Energy Harvesting," in *Proc. IEEE International Conference on Computing and Communication Systems (I3CS)*, Shillong, India, May. 2023, pp. 1-6.
[18] C. Zhai et al., "Wireless Powered Cooperative NOMA With Alamouti Coding and Selection Relaying," *IEEE Trans. Mob. Comput.*, vol. 23, no. 2, pp. 1366-1381, jul. 2024.
[19] V. N. Vo et al., "Performance optimization for hybrid TS/PS SWIPT UAV in cooperative NOMA IoT networks," *ELSEVIER, Alexandria Engineering*, no. 107, pp. 559–567, jul. 2024.
[20] M. Bakshi, B. Lall and R. K. Mallik, "Performance of Full-Duplex Cooperative NOMA Network With Direct Link And Battery-Assisted Non-Linear Energy Harvesting Near User," in *Proc. IEEE Open Journal of the Communications Society (COMMSOC)*, New Delhi, India, Jun. 2024, pp. 1-19.
[21] Q. S. Ahmad et al., "Achievable Sum Rate Analysis for Moving Relay Assisted Cooperative NOMA System Over Rician Fading Channels," *IEEE Access*, vol. 13, pp. 29778-29788, Feb. 2025.
[22] M. Cheng et al., "Outage Probability Analysis of Cooperative NOMA With Successive Refinement, " *IEEE Trans. Broadcast.*, vol. 71, no. 1, pp. 42-51, Mar. 2025.
[23] R. Bajpai et al., "Wireless Powered NOMA Assisted Full-Duplex Cooperative U2U Communications System With Fluctuating Two-Ray Channel," *IEEE Access*, vol. 13, pp. 54068-54079, Apr. 2025.
[24] H. Q. Ta et al., "Zero-Outage Secrecy in Short Packet IoT-Aided Cellular Cooperative Network With EH-NOMA," *IEEE Access*, vol. 13, pp. 75235-75245, May. 2025.
[25] Y. He et al., "Outage Probability Analysis of MISO-NOMA Downlink Communications in UAV-Assisted Agri-IoT With SWIPT and TAS Enhancement," *IEEE Trans. Veh. Technol.*, vol. 12, no. 4, pp. 2151-2164, Apr. 2025.
[26] M. M Salim et al., "Cooperative NOMA Meets Emerging Technologies: A Survey for Next-Generation Wireless Networks ," arXiv preprint arXiv:2505.16327, May. 2025.
[27] T. Li et al., "Design of Relay Selection Schemes for Uplink Cooperative NOMA Over Nakagami-m Fading," *IEEE Trans. Veh. Technol.*, vol. 12, no. 4, pp. 1-15, Jan. 2025.
[28] G. W. Machani and T. Malingo, "Cooperative Spectrum Sensing and Sharing in PD-NOMA Cognitive Radio Networks," *IEEE Access*, vol. 14, no.2, pp. 2592-2606, Jan. 2026.
[29] Z. Yang et al., "Delay and Energy Minimization for Cooperative NOMA-MEC Networks With SWIPT Aided by RIS," *IEEE Trans. Veh. Technol.*, vol. 73, no. 4, pp. 5321-5334, Apr. 2024.
[30] B.P. Chaudhary and R. K. MishraN, "Performance Analysis of SWIPT Cooperative-NOMA Over Rayleigh Fading Channel," in *Proc. IEEE International Conference on Computer and Automation Engineering (ICCAE)*, Sydney, Australia, May. 2023, pp.78-85.
[31] X. Qin et al., "Deep-Reinforcement-Learning-Based Uplink Security Enhancement for STAR-RIS-Assisted NOMA Systems With Dual Eavesdroppers," *IEEE Internet Things J.*, vol. 11, no. 17, pp. 28050-28063, Sept. 2024.
[32] T. Nimi, A. Babu, "Full-Duplex Cooperative NOMA Network with Multiple Eavesdroppers and Non-ideal System Imperfections: Analysis of Physical Layer Security and Validation Using Deep Learning," *IEEE Trans. Veh. Technol.*, vol. 12, pp. 1-16, Jul. 2024.
[33] V. N. Nayak et al., "Joint Covert and Secure Communication for SWIPT Assisted CNOMA Systems," in *Proc. IEEE Internet of Things Journal*, Visakhapatnam, India, Feb. 2025, pp. 1-13.
[34] R. Bajpai et al., "NOMA and Millimeter-Wave-Assisted SWIPT for Full-Duplex Cooperative D2D Communications," *IEEE Access*, vol. 13, pp. 42254-42261, Feb. 2025.
[35] N. Ashraf et al., "Performance Analysis of SWIPT-Assisted Cooperative NOMA Network With Non-Linear EH, Interference, and Imperfect SIC," *IEEE Access*, vol. 13, pp. 77481-77492, Apr. 2025.
[36] H. Q. Tran et al., "A Comprehensive Analytical Framework under Practical Constraints for a Cooperative NOMA System Empowered by SWIPT IoT," *Mathematics*, vol. 25, no. 4, pp. 1-15, 2024.
[37] K. Wang and M. Cheng, "Successive Refinement Coding and SWIPT for Energy-Efficient Cooperative NOMA Systems," *IEEE Trans. Broadcast.*, vol. 72, no. 1, pp. 382-386, Mar. 2026.
[38] S. Lu et al., "Outage Performance of a Dual-Layer Satellite–Terrestrial Communication System With Cooperative NOMA," *IEEE Trans. Veh. Technol.*, vol. 75, no. 1, Aug. 2026, pp. 1683-1688.
[39] S.D Roy et al., "Secrecy Outage Analysis of Energy Harvesting Enabled Two User Cooperative NOMA," in *Proc. IEEE International Conference on Recent Advances in Information Technology (RAIT)*, Dhanbad, India, May. 2023, pp. 1-6.
[40] B. Zhuo et al., "Partial-NOMA Based Physical Layer Security: Forwarding Design and Secrecy Analysis," *IEEE Trans. Intell. Transp. Syst.*, vol. 24, no. 7, pp. 7471-7484, Jul. 2023.
[41] V. N. Nayak et al., "SOP Minimization in Cooperative Relay-Based NOMA Network with Control Jammer," in *Proc. IEEE Wireless Antenna and Microwave Symposium (WAMS)*, Visakhapatnam, India, May. 2024, pp. 1-6.
[42] B. Jain et al., "Secrecy Outage Probability of NOMA Network under Amplify and Forward Scheme," in *Proc. IEEE International Conference on Device Intelligence, Computing and Communication Technologies, (DICCT)*, Dehradun, India, May. 2023, pp. 1-6.
[43] W. Guo, X. Wang, "Power Allocation for Secure NOMA Network Based on Q-Learning," *IEEE Access*, vol. 12, pp. 58454-58472, Apr. 2024.
[44] T. T. Nguyen et al., "A Low-Complexity Relaying Protocol for Cooperative Short-Packet NOMA-Based Spectrum Sharing Systems," *IEEE Trans. Veh. Technol.*, vol. 73, no. 6, pp. 9044-9049, Jun. 2024.
[45] K. K. Godugu, S. Vappangi, "Investigations on Secrecy Performance of Downlink Overlay CR-NOMA System With SIC Imperfection," *IEEE Access*, vol. 12, pp. 18051-18072, Feb. 2024.
[46] Y. Pei et al., "Secrecy Outage Probability Analysis for Downlink RIS-NOMA Networks With On-Off Control," *IEEE Trans. Veh. Technol.*, vol. 72, no. 9, pp. 7471-7484, Jul. 2024.
[47] I. Gradshteyn and M. Ryzhik, Tables of Integrals, Series, and Products, 7th ed. New York, NY, USA: Academic Press, 2007.



Opel N. Mbanzabugabo received a B.S. in Electrical and Electronics Engineering from the University of Rwanda in 2004 and an M.S. in Internet Systems from Kigali Independent University in 2021. He is pursuing a Ph.D. degree in Internet of Things at the University of Rwanda. As a temporary staff member, he served as an assistant lecturer at the University of Rwanda (2005), where he taught a course in digital communication. He is currently at Mobile Telephone Network (MTN) Rwanda as Acting Access Network Regional Manager. Previously, as a Senior Engineer at MTN, he deployed, optimized, and maintained the good functionality of 2G, 3G, 4G, and 5G in both radio and transmission. His research interests, as a Ph.d student, include cooperative non-orthogonal multiple access (C-NOMA), energy harvesting in vehicular communication, Artificial intelligence (Deep Reinforcement Learning and Soft Actor Critic) and next-generation wireless network systems.



Charles Kabiri received his B.S. degree in Electrical and Electronics Engineering from the National University of Rwanda in 2006, and his M.S. degree in Information and Communication Systems in 2010 from Huazhong University of Science and Technology, Wuhan, China. He obtained his Ph.D. degree in Telecommunication Systems in April 2015 from Blekinge Institute of Technology, Faculty of Computing, Karlskrona, Sweden. He worked at CIMERWA Ltd as an electrical and maintenance engineer since early 2007, before joining the Faculty of Applied Sciences at the National University of Rwanda in August 2007. He was a Junior Associate at the Abdus Salam International Center for Theoretical Physics, Trieste, Italy from 2012 until 2017. He is currently an Associate Professor of Telecommunication Systems and Deputy Dean of the School of Engineering, College of Science and Technology, University of Rwanda, Rwanda. His research interests are in the areas of radio communication systems and renewable energy.



Kayalvizhi Jayavel serves as a Senior Lecturer and Course Leader for the BSc Data Science and AI programme at the Creative Computing Institute, University of the Arts London, UK, bringing more than 25 years of experience in academia and research. In recognition of her significant contributions to teaching and research, she has been conferred the title of Associate Honorary Professor by the College of Science and Technology at the University of Rwanda. She has also held senior administrative positions focused on international policy and strategic collaboration, notably as Assistant Director of International Relations at SRM Institute of Science and Technology, India. A Fellow of the Higher Education Academy (UK), she holds a PhD in Computer Science, with research interests spanning data-driven IoT systems and applied artificial intelligence across multiple domains. She has led and contributed to international projects in AI, IoT, healthcare, precision agriculture, and digital equity, collaborating with partners across Europe, Africa, and Asia. Her scholarly contributions include numerous publications in reputed journals and conferences, alongside service as an editor and reviewer for leading academic outlets. She has received widespread recognition for excellence in teaching and mentorship, as well as for her advocacy for women in technology and inclusive education.



Louis Sibomana is currently the Head of Science, Technology Development and Outreach Department at the National Council for Science and Technology (NCST), Rwanda, and Honorary researcher and Senior lecturer at the School of Engineering, College of Science and Technology, University of Rwanda. Louis is Certified Project Management Professional with experience, skills and knowledge in leading and managing projects and cross-functional teams. He is skilled with senior administrative leadership, policy and strategies analysis and development, and with proven background in research, teaching and educational programs development and management, supervision and mentorship, as well as effective partnership and collaboration with various stakeholders. Research interests include performance analysis of wireless communication, and applications of emerging technologies such as Internet of Things and Artificial Intelligence in various sectors. Dr. Louis is involved in different research projects and has published several papers in both international and peer reviewed journal articles.

CONTENTS PAGE